Nancy McGuire in Noteworthy Chemistry (ACS) Autumn 2013

http://www.acs.org/content/acs/en/noteworthy-chemistry/archive/november-25.html#nc4

November 25, 2013

Processing conditions affect graphene surface contamination and lattice defects. Graphene, a 2-D material that shows promise for a variety of electronics applications, is commonly prepared by exfoliating single carbon layers from bulk graphite. Mechanical exfoliation produces small amounts of highly pure graphene, whereas harsh chemical exfoliation produces larger amounts of graphene contaminated with oxides and amorphous carbon.

Milder chemical processes, coupled with ultrasonication, require stabilizing additives to prevent re-aggregation. Noncovalent stabilizers are preferable to covalent ones because they do not saturate the carbon–carbon bonds in the graphene layer.

N. Tagmatarchis and coauthors at the National Hellenic Research Foundation (Athens), the University of Antwerp (Belgium), and the University of Mons (Belgium) studied the effects of ultrasonication duration and power levels on the introduction of foreign species onto the graphene surface. They produced the highest concentrations of exfoliated graphene by tip ultrasonication at 60 min and 40 W. *o*-Dichlorobenzene (*o*-DCB) was a more efficient exfoliant than *N*-methyl-2-pyrrolidone (NMP).

A comparison of the Raman spectra of intact graphite and the exfoliated graphene showed that *o*-DCB and NMP promote exfoliation by physical processes rather than electronic interactions. The spectra also indicated that the graphene sheets were oligolayers rather than monolayers and that the graphene lattice contained sp^3-hybridized carbon atoms that were bonded to oxygenated substituents. Thermal, attenuated total reflectance IR, and X-ray photoelectron spectroscopy (XPS) studies confirmed this and provided additional information about the concentration and identities of the foreign species.

Ultrasonication in NMP produced exfoliated graphene containing more oxygen than did *o*-DCB. The concentration of oxygen species was sensitive to ultrasonication power but not duration. With *o*-DCB, the oxygen content can be reduced by increasing the duration or the power. XPS showed the presence of carboxylic acids, ethers, and epoxides, but not carbonyl groups, which suggests that the oxygen-containing groups are produced by exposure to air, not to the solvent.

Increasing the power and/or duration of the ultrasonication appears to decompose some portion of the oxygenated species, but it also introduces defects into the graphene sheet. It is possible that sonication treatment further separates the oligolayered graphene flakes, but the authors could not verify this by using XPS analysis. *(J. Phys. Chem. C* **2013,** *117,* 23272–23278; Nancy McGuire)

http://www.acs.org/content/acs/en/noteworthy-chemistry/archive/november-18.html#nc1

November 18, 2013

Natural wetland remediates acidic mine drainage. A. P. Dean and co-workers at the University of Manchester (UK) conducted a 14-year evaluation of a natural wetland along the southern Afon Goch river system (Anglesey, North Wales, UK) between the Parys Mountain copper mine and the Irish Sea (see map). They measured its ability to remediate highly acidic mine drainage (AMD). This well-established wetland has existed since the 1890s or earlier.

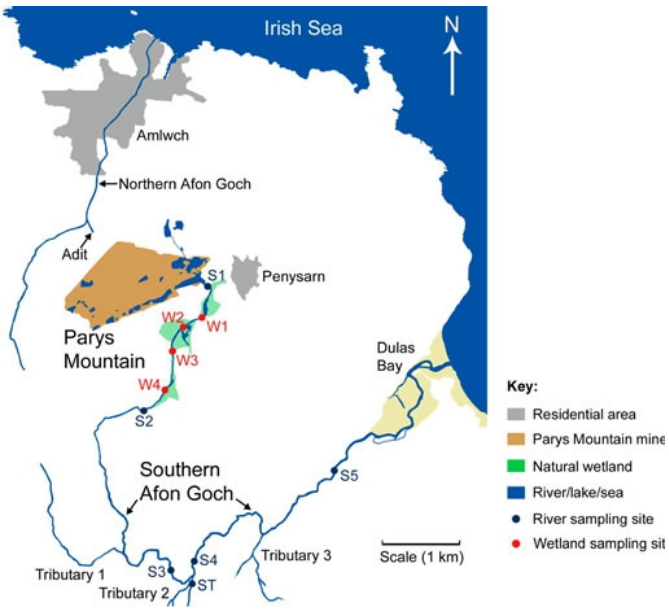

The Parys Mountain mine was in continuous operation from the mid-18th century until 1911. It continues to discharge more copper and zinc to the Irish Sea than any other source. The discharges also account for the largest proportion of the total iron release nationally.

Natural wetlands may be highly effective for remediating AMD because they have adapted to the low-pH, high-metal environment of an AMD-polluted system over a long time. There are, however, no reported long-term evaluations of natural wetland remediation performance; and the biological composition and diversity of natural AMD wetlands are poorly understood.

Previous studies of natural wetlands indicated that they might release metal contamination downstream, but those studies were shorter in duration than this one. Although seasonal changes were not examined in this study, changes in flow rates were incorporated. Limitations in data collection prevented a full mass balance analysis in this study, but the data show that this wetland acts as a net sink for all dissolved metals before and after drainage diversion.

Between 1997 and 2010, the researchers sampled one upstream site, four downstream sites, and a control site. They sampled six sites in the wetland region (including two of the earlier sites) twice in the autumn of 2011.

Before 2003, the wetland retained 55, 64, and 37% of the dissolved iron, zinc, and copper runoff from the mine. In 2003, to reduce flood risk, the drainage from the mine was diverted from the southern Afon Goch to the northern Afon Goch, thereby decreasing the load on the wetland and allowing it to reduce the downstream metal content by 83−94%.

An associated pH increase from 2.7 to 5.5 (compared with 6.2 at the control site) provided long-term improvements to the downstream benthic invertebrate community. Invertebrate fauna sampling from 2008 on showed an increase in diversity, including pollution-intolerant taxa, at sites downstream from the wetland.

Although plant roots played a part in retaining dissolved metals, the main metal accumulation was in the sediment. Plant and microbial activity increases groundwater pH, which promotes precipitation of metal salts and complexation of metal ions with organic ligands in the sediment. Thus, multiple interacting processes created an efficient, self-sustaining AMD remediation site in this wetland region. (*Environ. Sci. Technol.* **2013,** *47,* 12029–12036; Nancy McGuire)

http://www.acs.org/content/acs/en/noteworthy-chemistry/archive/november-11.html#nc3

November 11, 2013

Use materials science techniques to study pathological crystals. Crystal formation within the human body causes a variety of medical problems. Pathology research typically focuses on the physiological rather than the materials science aspect of this phenomenon. Studies of basic crystal properties such as nucleation, growth, aggregation, and adhesion under pathological conditions may help identify causes, therapies, and preventive measures.

L. N. Poloni and M. D. Ward* of New York University (New York City) reviewed the literature on crystal formation in simulated physiological environments. They summarized the current knowledge of the roles of urinary substituents, anionic proteins, synthetic polymers, and small molecules in the formation of kidney stones, gallstones, gout-forming sodium urate crystals, and cholesterol crystals.

Advances in analytical techniques, including grazing incidence X-ray diffraction and cryogenic soft X-ray tomography, offer insight into crystal-growth modes and kinetics at the near-molecular scale. Chemical force microscopy provides information about the adhesive properties of individual crystal faces by using functionalized probes to measure interactions between the crystal surfaces and specific molecular entities.

In situ atomic force microscopy gives a molecular-level view of crystal growth in real time and under variable conditions of composition, temperature, pH, and solution flow rate. This knowledge is vital for developing inhibitors that stereospecifically bind to growing crystal faces and retard further growth.

The authors believe that additional studies can advance the knowledge of crystallization-like processes, including the formation of amyloid proteins associated with neurodegenerative diseases. Substances that interfere with the *Plasmodium falciparum* malaria parasite's ability to crystallize free heme may be used to overcome this parasite's resistance to antimalarial drugs. Similar studies may also help prevent the unwanted crystallization of pharmacological compounds inside the body. (*Chem. Mater.* **2013,** *25,* Article ASAP; Nancy McGuire)

http://www.acs.org/content/acs/en/noteworthy-chemistry/archive/november-4.html#nc3

November 4, 2013

Capture nanoparticle and virus images with a smart phone. Detecting single nanoparticles, microbes, and tagging-agent molecules in the field could be useful in biomedicine, environmental and food inspection, forensic analysis, epidemiology, and detection of counterfeit and contraband products. Optical imaging and spectroscopy of single nanosized objects typically require complex, expensive experimental setups in a controlled laboratory environment. A field instrument for this type of work would open new applications and allow single-object detection and analysis when access to large laboratory facilities is not available or affordable.

As a first step toward this goal, A. Ozcan and colleagues at the University of California, Los Angeles, built a fluorescence imaging system that can be mounted on a smart phone. It uses a diode laser source and a lens coupled with a long-pass thin-film interference filter to collect the fluorescence signal from a 0.6 mm x 0.6 mm area of the sample, which is inserted into the device on a sliding tray.

For larger, strongly fluorescing objects that are relatively insensitive to imaging and focus conditions, the field of view can cover the entire 3 mm x 3 mm sample area. The angle between the laser beam and the sample is ≈15°, which reduces the background noise at the detector. The smart phone's camera serves as a detector, and a translation stage allows focus adjustment. The researchers used a 3-D laser printer to fashion a lightweight holder for mounting the optical components onto the smart phone.

This version of the device has a spatial resolution of ≈1.5 μm and the ability to detect objects labeled with a few hundred fluorophores. The authors demonstrated their device by using 100-nm dye-doped polystyrene beads and dye-labeled human cytomegaloviruses. They validated their results by using conventional optical and electron microscopy.

S. Khatua and M. Orrit at the Leiden Institute of Physics (The Netherlands) wrote a perspective (*ACS Nano* **7,** 8340–8343) on this device, in which they explored potential applications and recommended directions for future development. (*ACS Nano* **2013,** *7,* 9147–9155; Nancy McGuire)

http://www.acs.org/content/acs/en/noteworthy-chemistry/archive/october-28.html#nc5

October 28, 2013

Silicon nanowires form flexible, transparent, free-standing sheets. Current flexible, transparent electronic-device components are largely the domain of organic light-emitting diodes, but these materials are expensive and have limited life spans. Silicon, the mainstay of the conventional semiconductor industry, is brittle and opaque at the macro scale; but it becomes highly flexible at the nanoscale. Nanostructured silicon may be used in applications such as flexible, touch-sensitive display screens and wearable electronic devices.

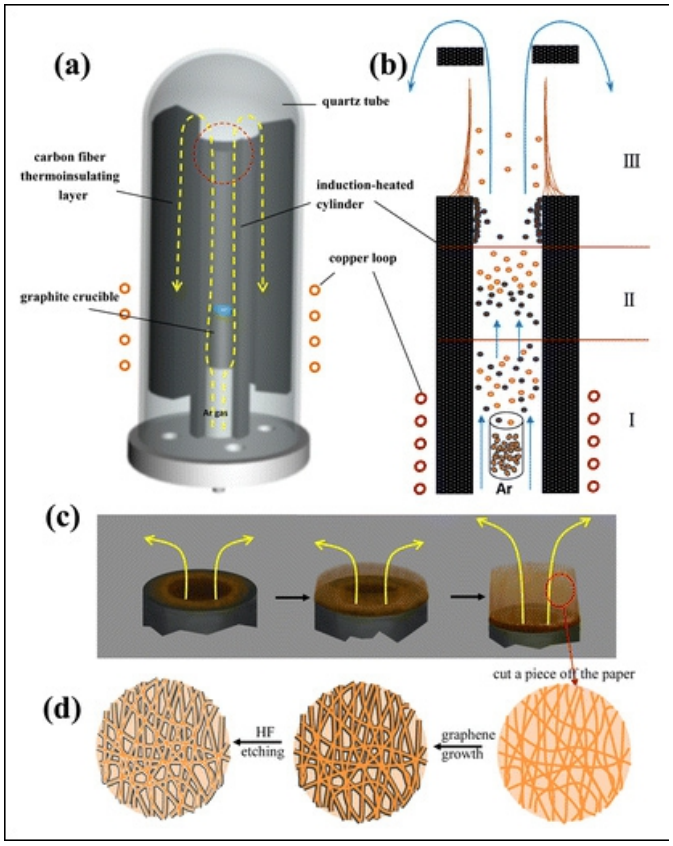

C. Wang and co-workers at Sun Yat-sen (Zhongshan) University (Guangzhou, China) developed a simple method for making free-standing sheets of interlocking 10-nm–diam silicon nanowires. They heated metastable SiO powder in a vertical high-frequency induction furnace at 1600 ºC under a stream of high-purity argon for 1 h [(a) in the figure]. The carrier gas transports the resulting silicon and SiO_2 vapors to the low-temperature zone of the graphite furnace tube. The denser SiO_2 forms a powder on the upper inner wall of the tube. The silicon vapor is carried to the upper opening of the tube, where it forms nanowires [(b) and (c) in the figure].

Because the authors found no evidence of metal catalysts or impurities on the tips of the nanowire nuclei, they believe that the growth of the nanowires is assisted by a small amount of SiO_2 that forms a matrix at the opening of the tube.

Each wire consists of a crystalline core surrounded by an amorphous sheath. The carrier gas orients the nanowires in the direction of the gas flow, and the wires spontaneously interlock with each other as they grow.

This process forms a self-supporting cylindrical network structure ≈2 cm high and ≈2 cm diam. The sheets are flexible, transparent, and highly porous; and they could serve as hosts to other functional materials.

Coating the nanowires with graphene [(d) in the figure] produces flexible, transparent lithium-ion battery electrodes with excellent lithium-storage performance, high storage capacity, and good cycling stability. The graphene sheaths insulate the nanowires from direct contact with the electrolyte. Graphene gives a slightly black color to the sheets, but it does not block light transmittance significantly. After the residual SiO_2 is removed with HF, there is ample space between the silicon nanowires and their graphene sheaths to allow the nanowires to expand during lithiation. (*Nano Lett.* **2013,** *13,* 4708–4714; Nancy McGuire)

http://www.acs.org/content/acs/en/noteworthy-chemistry/archive/october-21.html#nc1
October 21, 2013

A Vietnamese starfish produces anti-inflammatory compounds. Starfish historically have been used in Vietnamese folk medicines and medicinal foods. There are no reports, however, of the chemical constituents and biological activity of the common edible starfish *Astropecten monacanthus*. A recent investigation uncovered a series of asterosaponins from this starfish that have significant anti-inflammatory activity.

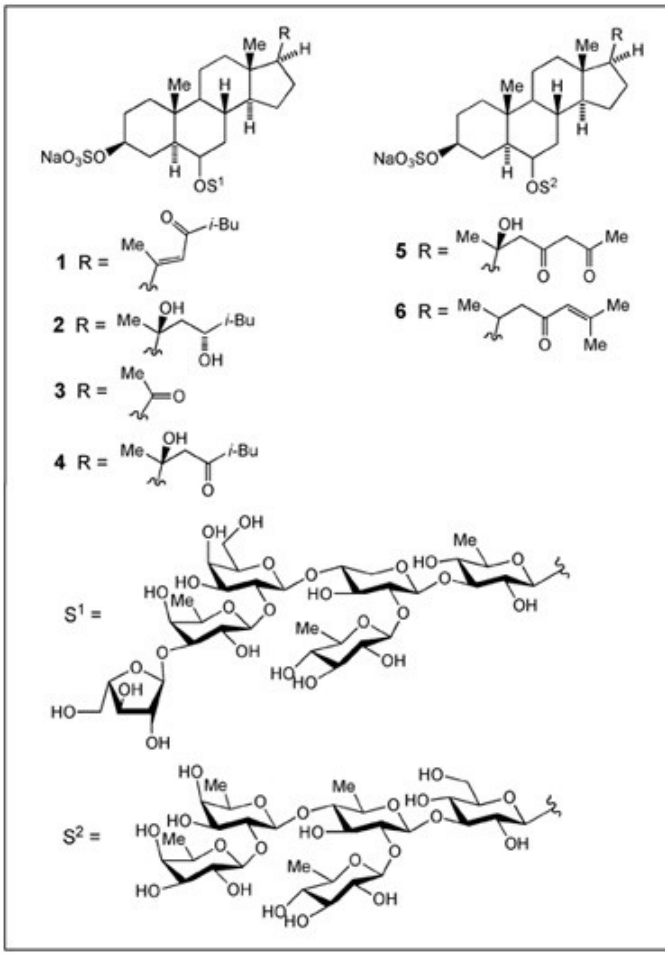

C. V. Minh, Y. H. Kim, and coauthors at the Vietnam Academy of Science and Technology (Hanoi), Chungnam National University (Daejeon, Korea), Jeju National University (Korea), and Nhatrang Institute of Technology Research and Application (Vietnam) extracted *A. monacanthus* with MeOH. They then suspended the extract in water and successively partitioned it with EtOAc and *n*-BuOH. They chromatographically separated the *n*-BuOH fraction to produce the six asterosaponin compounds shown in the figure.

The previously known compounds psilasteroside (**4**) and marthasteroside (**6**) were identified by their physical and spectroscopic properties. The authors characterized compounds **1**, **2**, **3**, and **5** by using Fourier transform cyclotron resonance MS and ^{1}H and ^{13}C NMR. Compounds **1**, **2**, and **4** contain the same oligosaccharide chain. Compounds **1**–**4** have the same steroidal nucleus but different side chains. Compounds **5** and **6** have similar steroidal nuclei and pentasaccharide chains but different side chains.

The authors evaluated the anti-inflammatory effects of the MeOH extract and *n*-BuOH fractions by measuring the production of the pro-inflammatory cytokines IL-12 p40, IL-6, and TNF-α in lipopolysaccharide-stimulated bone marrow–derived dendritic cells, with the following results:

- Compound **5** has potent inhibitory effects on all three cytokines.
- Compounds **1** and **6** significantly inhibit IL-6 production.
- Compound **3** shows moderate inhibitory effects on IL-6 production.
- Compounds **2** and **4** do not significantly reduce any of the three pro-inflammatory cytokines.

In vivo testing is required to ascertain whether the asterosaponin compounds retain their bioactivity after oral ingestion or if they are inactivated by the rapid cleavage of the oligosaccharide chains. (*J. Nat. Prod.* **2013,** *76,* 1764–1770; Nancy McGuire)

http://www.acs.org/content/acs/en/noteworthy-chemistry/archive/october-14.html#nc5

October 14, 2013

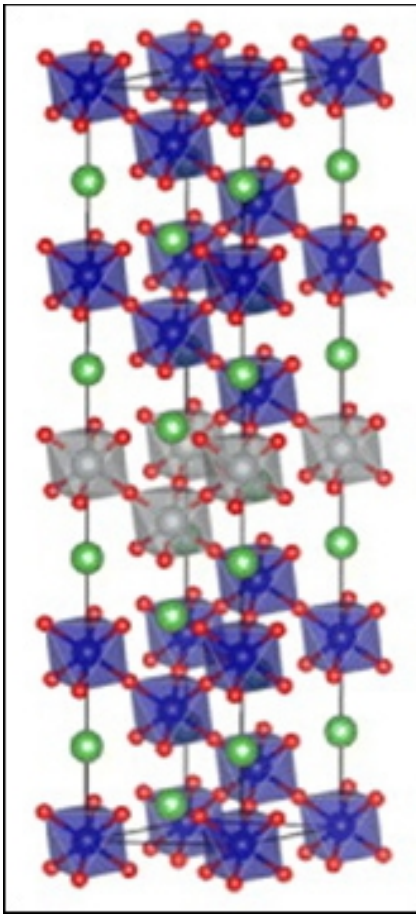

Layered perovskites might form room-temperature spintronic devices, according to a theoretical study. Q.-F. Liang, L.-H. Wu, and X. Hu* at the National Institute for Materials Science (Tsukuba, Japan) and Shaoxing University (China) propose fine-tuning the degrees of freedom of electron spin, sublattices, and valleys (conduction band minima) in perovskite G–type antiferromagnetic insulators. These materials would be grown along the [111] direction and achieve a new topological insulator state. (In G-type ordering, two sublattices have spins that are antiparallel to each other.)

Bulk topological insulators are insulating, but their quantum-edge states can transport current with no dissipation. These states are realized only at low temperatures, at which the edge-state spin-up and spin-down electrons are mixed. This study indicates that an antiferromagnetic insulating state with a reversible spin-polarized quantum edge current can be achieved at room temperature or higher by tuning a combination of the electric potential, antiferromagnetic field, and spin–orbit coupling.

The researchers were inspired by the quantum spin Hall effect seen in graphene and other materials with honeycomb-like crystal lattices. They extended the concept to perovskite insulators ABO_3 in which magnetic B atoms exhibit G-type antiferromagnetic ordering and are arranged in buckled honeycomb lattices along the [111] direction. The figure shows a six-layer ABB′X perovskite with one layer of B (blue) replaced by B′ (gray).

Replacing one layer of magnetic B atoms with a layer of nonmagnetic B′ atoms and applying a uniform electric field induce a staggered electric potential for the two sublattices. The G-type antiferromagnetic ordering of the B atoms on either side of the B′ layer provides an antiferromagnetic exchange field.

The authors performed first-principles calculations on a model solid that consisted of six layers of $LaCrO_3$ with one layer of $La_2Ag_2O_6$ or $La_2Au_2O_6$ sandwiched into the center. They estimated a spin–orbit coupling of several tens of meV, which makes this new topological state available at room temperature. Recent developments in laser molecular beam epitaxy allow the growth of perovskite structures along the [111] direction with atomic precision, so that verifying the calculations in the lab should be feasible. (*New J. Phys.* **2013,** *15,* No. 063031; Nancy McGuire)

http://www.acs.org/content/acs/en/noteworthy-chemistry/archive/october-7.html#nc1

October 7, 2013

This soy-based alkyd coating resists corrosion and bacteria. The quest continues for low–volatile organic compound (VOC), high-performance surface coatings that do not rely on petroleum feedstocks. Antibacterial coatings are of particular interest to the food and medical-device industries.

Alkyd resins—oil-modified polyesters—are used as coatings because of their high gloss, solvent resistance, and low cost. Conventional methods for producing these resins involve organic solvents that release unacceptable levels of VOCs into the atmosphere. Waterborne alkyds release almost no VOCs, but they dry more slowly than their oil-based counterparts, and they are not as resistant to water, acids, and bases.

S. Pathan and S. Ahmad* at the National Islamic University (New Delhi, India) synthesized soy-based alkyd coatings modified with butylated melamine formaldehyde (BMF). Their flexible adhesive coatings are highly scratch-resistant and withstand impacts of >150 lb/in. (>26.8 kg/cm). The coatings are antibacterial and corrosion-resistant. They are safe to use at temperatures as high as 200 °C.

Pathan and Ahmad treated soy oil (**1**) and glycerol (**2**) with NaOH under nitrogen to produce soy monoglyceride (**3**), which was then treated with phthalic anhydride (**4**) to produce the soy alkyd (**5**). The alkyd was neutralized with Et_3N to make it "waterborne" (**6**). [*It is not clear in the article whether "waterborne" means water-soluble.—Ed.*]

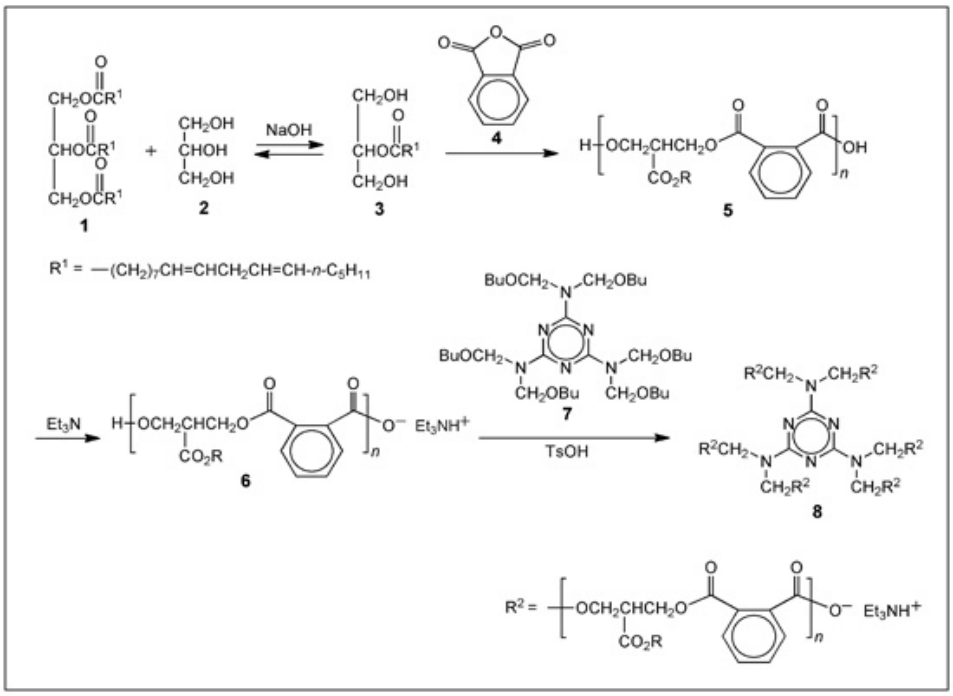

Finally, the authors dissolved **6** and BMF (**7**) in various ratios in aq MeOH. With *p*-toluenesulfonic acid (TsOH) as the catalyst, they produced 3-D thermoset polymers (**8**).

Incorporating BMF into the soy alkyd increases the hydrophobicity of the coatings, which promotes corrosion resistance. The coatings protected the substrates against acid, alkaline, and tap-water corrosion. Adding BMF also increases the antibacterial activity of the soy alkyd, particularly against *Staphylococcus aureus* (and to a lesser extent, *Escherichia coli*), a useful feature for food-packaging materials. (*ACS Sustainable Chem. Eng.* **2013,** *1,* Article ASAP; Nancy McGuire)

http://www.acs.org/content/acs/en/noteworthy-chemistry/archive/september-30.html#nc5

September 30, 2013

"**Legacy" mercury limits benefits from closing down smelters.** For 80 years, Manitoba's Flin Flon copper smelter (see figure) was Canada's largest point source of mercury emissions. The smelter was closed in 2010, but its legacy lives on in the air, water, and soil.

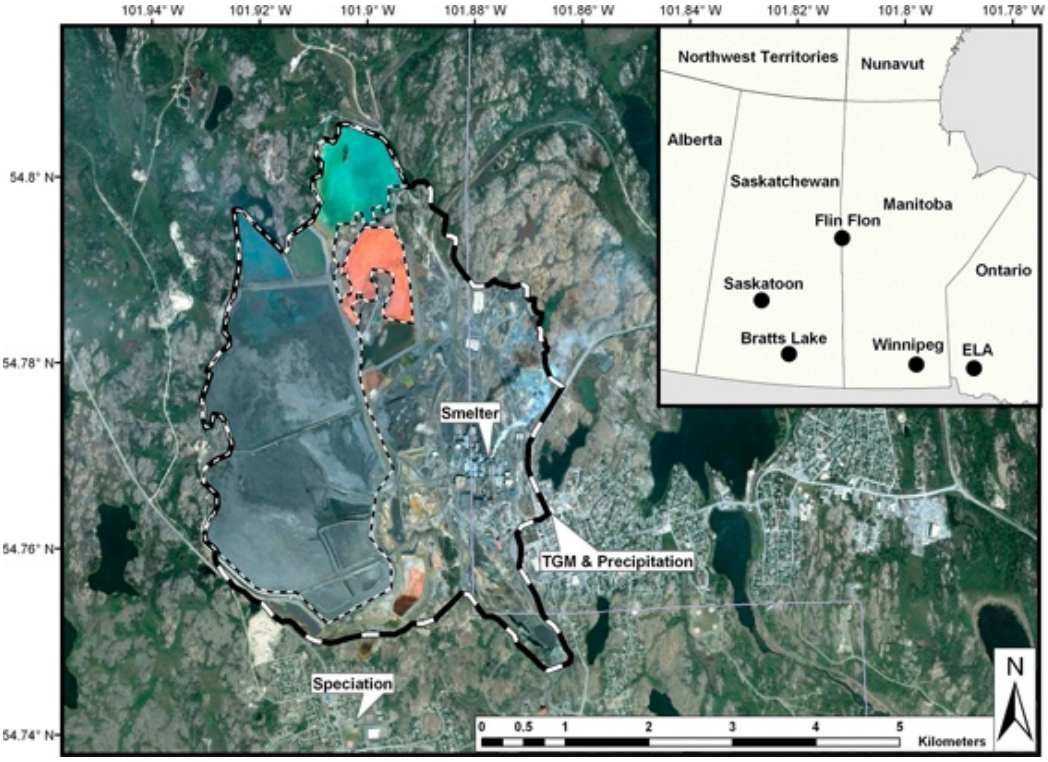

C. S. Eckley, M. T. Parsons, and colleagues at Environment Canada (Toronto; Edmonton, AB; and Dartmouth, NS), the US Environmental Protection Agency (Seattle, WA), and the University of Alberta (Edmonton) measured total gaseous mercury (TGM) in the air, mercury in precipitation, and ancillary parameters in the area around the smelter to assess any lingering effects on the environment.

The Flin Flon smelter is an ideal case study because data could be collected before and after the smelter closed and because the nearest industrial releases of any significance are >450 km to the southwest in Saskatoon, SA. While the smelter was operating, TGM levels (4.1 ± 3.7 ng/m^3) in the air near the smelter were ≈3-fold greater than those at other Canadian monitoring stations. They decreased 20% during the year after it closed and have remained at twice the background levels since then. Concentrations before and after closure were highly variable, and there were frequent concentration peaks. Similar trends were observed for mercury in precipitation.

Evidence indicates that contaminated soil and tailings, which were the largest contributors to local TGM concentrations during and after smelter operations, are re-emitting mercury into the air. During smelter operations, stack emissions were a more significant contribution to the regional and global mercury pool.

After the smelter closed, the absolute magnitude of surface-air TGM flux decreased, but it contributed more on a percentage basis to the TGM in the air. The authors make no estimate of how long the soil and tailings will continue to re-emit mercury into the air, and they recommend further investigation. (*Environ. Sci. Technol.* **2013,** *47,* 10339–10348; Nancy McGuire)

http://www.acs.org/content/acs/en/noteworthy-chemistry/archive/september-16.html#nc6

September 16, 2013

Coated graphene quantum dots shine on and on in vivo. Medical imaging agents that are based on photoluminescent inorganic semiconductor quantum dots (QDs) give higher quantum yields and less photobleaching than organic dyes. The QDs. however, tend to ionize in vivo, causing toxic side effects.

Photoluminescent graphene quantum dots (GQDs) are less toxic, but the uncoated GQDs rapidly lose their photoluminescence. Coating the GQDs preserves their photoluminescence, improves their stability in water, and further reduces their toxicity.

Y.-k. Lee and co-workers at the Korea National University of Transportation (Chungju) investigated GQDs coated with polydopamine (pDA), a derivative of the adhesive compound 3,4-dihydroxyphenylalanine (DOPA) used by mussels. A previous study (Hong, S., et al. *Nanomedicine* **2011,** *6,* 793–801) showed that pDA coatings greatly reduce inflammatory and immunological responses to QDs in the bloodstream.

The authors observed pDA-coated and uncoated GQDs in pH buffer solutions (pH 5, 7, 9, and 11) and in a 2% NaCl solution over a period of 14 days. The uncoated GQDs lost 45% of their photoluminescence in the pH 5 and 7 solutions over this period, possibly because protons interacted with the negatively charged GQDs. All of the coated GQDs retained their photoluminescence over the test period. Increasing particle size promoted aggregation but did not cause the GQDs to precipitate.

The researchers tested cytotoxicity toward KB cancer cells in vitro. The cells took up both coated and uncoated QDs, and a green photoluminescence was observed from the cytoplasm and the cell membrane. The uncoated QDs were only slightly toxic; the authors attribute this to large amounts of adsorbed oxygen, which acts as a coating. pDA-coated GQDs had no detectable toxicity.

The authors injected coated and uncoated GQDs into nude mice to observe the biodistribution of the particles and the duration of the photoluminescence. The figure shows optical images of nude mice and their isolated organs: (a) saline-treated control mice; (b) uncoated GQD–treated mice; (c–e) mice treated with GQDs coated with dopamine polymerized for 3, 6, and 12 h, respectively; and (f) photoluminescence intensities of organ tissues after treatment with coated and uncoated GQDs.

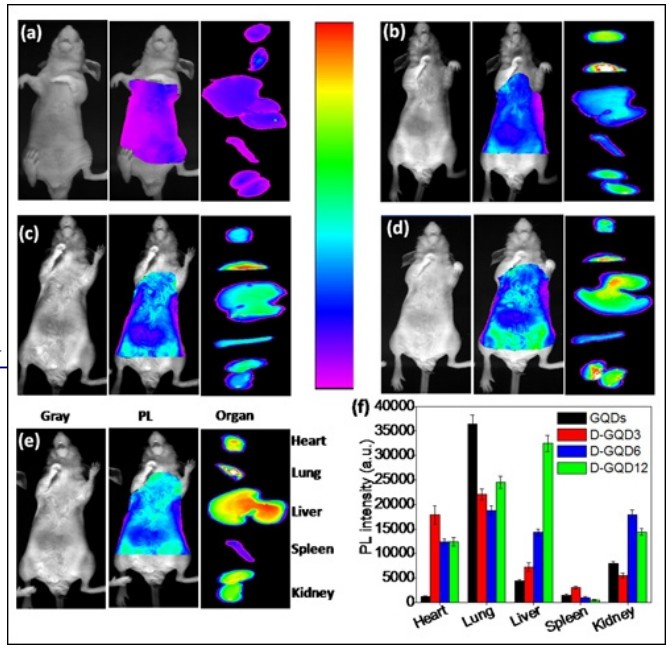

Both types of GQDs were distributed to all of the organs examined. Most of the uncoated GQDs in the size range 3–6 nm were expelled through the kidneys within 4 h of injection. Coated GQDs remained in the body longer, and showed stronger photoluminescence in all organs except the lungs. Increasing the particle size increases the photoluminescence in the liver, possibly because larger particles are not excreted as rapidly. (*ACS Appl. Mater. Interfaces* **2013,** *5,* 8246–8253; Nancy McGuire)

http://www.acs.org/content/acs/en/noteworthy-chemistry/archive/september-9.html#nc4

September 9, 2013

Thermosalient crystals relieve stress by jumping, spinning, or blowing themselves to bits. Thermosalient (TS) crystals (see examples) convert heat to mechanical energy, propelling themselves over distances thousands of times their own size in less than 1 ms. P. Naumov and co-workers at New York University Abu Dhabi (UAE) studied the thermodynamic, kinematic, structural, and macroscopic factors that drive these self-actuating crystals.

The researchers discovered a significant crystal-size effect on the differential scanning calorimetry profile and the temperature at which the TS phase transition occurs. Thermal cycling gradually reduces the force of the jumps, and the crystals eventually fragment and disintegrate. Grinding the crystals suppresses the TS transition, possibly because defects cannot form and propagate in crystals with less than a certain critical size.

In almost all cases, crystal symmetry is preserved across the phase transition. The unit-cell volumes show only modest expansion, ranging from 0.7% to 4.3%. Most of the crystals, however, show a marked expansion along one or two crystal axes, which is balanced by a reduction along the other axes.

The authors propose a two-stage process in which a small structural transformation causes a sufficient accumulation of internal strain to trigger a rapid second structural transformation that relieves the strain. Crystals that release strain gradually do not exhibit TS-type behavior.

The authors identified two main mechanisms for strain accumulation and release. The first applies to layered crystal structures composed of flat rigid molecules packed in layers that lack extended hydrogen bond networks or of layered molecular packings that saturate their hydrogen-bonding potential by dimerizing or polymerizing. These structures have limited degrees of freedom, and the molecules cannot rotate significantly. Heating or cooling produces anisotropic distortion, which introduces strain that eventually outweighs the weak cohesive interactions between the layers. This triggers a rapid sliding of the layers, manifested as crystal twinning and a change in unit-cell dimensions.

A second mechanism applies to crystals that have flexible bulky molecules composed of a central core bonded to multiple substituents that hinder hydrogen bonding between molecules. These molecules are more flexible and have more conformational freedom. Heating induces molecular torsion and

terminal-group rotation that produce strain. As the strain is released, the flexible molecules relax to their most stable conformation. After the phase transition, the molecular packing has the same relative orientation, but with increased intermolecular distances and increased conformational disorder of the terminal groups. (*J. Am. Chem. Soc.* **2013,** *135,* 12241–12251; Nancy McGuire)

http://www.acs.org/content/acs/en/noteworthy-chemistry/archive/september-2.html#nc2

September 3, 2013

Electrogenerated chemiluminescence detects peroxide explosives. The white solid triacetone triperoxide (TATP, at left in the figure) is one of the most sensitive explosives known—it can be set off by friction, heat, or impact. It was used in 2005 in the attack on the London public transportation system that killed 52 people and injured more than 700. Organic peroxide explosives, including TATP and hexamethylene triperoxide diamine (HMTD, at right in the figure), can be made from off-the-shelf ingredients, and they easily pass through common screening devices designed to detect nitrogen-based explosives.

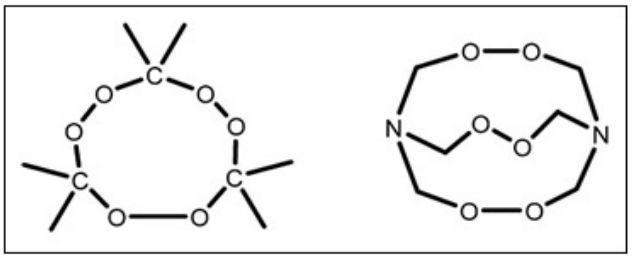

Several reliable methods exist for detecting peroxide-based explosives. Some, like MS, are very sensitive, but they are expensive and not well-suited to field testing. Ion mobility spectroscopy results are affected by temperature and moisture, and luminophore impurities hamper fluorescence testing. IR and UV–vis spectroscopy often require extensive sample preparation and are not sensitive to trace amounts of explosives.

S. Parajuli and W. Miao* of the University of Southern Mississippi (Hattiesburg) set out to develop a method for detecting trace amounts of organic peroxides that would be suitable for use at security checkpoints in mass-transit facilities and in forensic and environmental testing applications. They chose electrogenerated chemiluminescence (ECL) because of its selectivity, sensitivity, and rapid results.

The authors tested ECL's ability to detect and quantify TATP and to distinguish this compound from HMTD in a H_2O–MeCN solution containing a phosphate buffer and $Ru(bpy)_3^{2+}$ as an ECL emitter. TATP is sparingly soluble in water, but water is needed to produce hydroxyl radicals from the peroxide functional groups in TATP. MeCN is a better solvent, and it enhances the ECL intensity by stabilizing hydroxyl radicals in solution.

Cathodic potential scanning produces hydroxyl radicals. These oxidize electrogenerated $Ru(bpy)_3^{+}$ cations to form excited-state $Ru(bpy)_3^{2+*}$, which quickly reverts to $Ru(bpy)_3^{+}$, accompanied by photon emission.

This method’s TATP detection limit (2.5 μM) is 3 times lower than that of UV−vis detection and 400 times lower than that attainable with LC-IR. Results can be obtained in as little as 5 min.

Oxygen-based bleaches commonly found in laundry detergents could leave trace amounts of H_2O_2 on a traveler's clothing, creating false positives for TATP. Pretreating samples with a catalase enzyme, followed by enzyme deactivation with NaN_3, effectively suppresses ECL from this source.

TATP produces ECL upon cathodic potential scanning only, whereas HMTD produces ECL upon both cathodic and anodic potential scanning because of its tertiary amine functional groups. This difference can be used to distinguish between the two compounds. (*Anal. Chem.* **2013,** *85,* 8008–8015; Nancy McGuire)